Mechanical Properties and Microscopic Deformation of Unidirectionally Reinforced Plastics

A. Nakahira, S. Nishijima, M. Hussain, T. Okada and K. Niihara

ISIR Osaka University, 8-1 Mihogaoka, Ibaraki
Osaka 567, Japan

ABSTRACT

Some important mechanical properties, such as Young's modulus, hardness in transverse direction and interlaminar shear strength, of carbon fiber reinforced plastic and hybrid carbon fiber were investigated. A significant improvement of mechanical properties in the region of interface of matrix and carbon fiber was achieved by incorporation of 10 vol% Al_2O_3 filler, especially nano-size Al_2O_3 particulate into carbon fiber reinforced plastic. The deformation behavior of carbon fiber reinforced plastic and hybrid carbon fiber reinforced plastic was investigated by the micro indentation technique.

1. INTRODUCTION

Carbon fiber reinforced plastics (CFRPs) have been employed as the structural materials for aerospace and automobile applications because of their high specific strength and modulus /1-4/. CFRPs can also be used for radiotelescope antennae due to their high specific modulus as well as their dimensional stability /5/.

Although CFRP is a widely applicable advanced composite material, defects at the interface between matrix and reinforcement have a deleterious effect on its macroscopic properties. The difference in properties between matrix and reinforcement is especially large in CFRP and hence defects at the interface easily occur during the fabrication process, leading to poor mechanical and thermal properties of the CFRP /6/. The interface characteristics are therefore of great importance for a detailed evaluation of high-performance CFRP.

However, it is usually difficult to evaluate the interface characteristics because the characteristics of a composite change when the interface area is cut out of the composite, due to the change in the constraint condition. The interface properties of a composite reflect the constraint condition of reinforcement. For example, the interlaminar shear strength depends on the interfacial pressure from matrix to carbon fiber /7,8/. The constraint condition, therefore, would be one of the parameters of the interfacial condition. The constraint condition is thought to affect the apparent properties of reinforcement in a composite. Consequently, the apparent mechanical properties of the carbon fiber should be another parameter of the interface properties.

In this work the apparent mechanical properties of carbon fibers such as Young's modulus and hardness in a composite were measured. The interfacial properties, based on the apparent properties of the carbon reinforcement, are discussed.

2. EXPERIMENTAL PROCEDURE

2.1. Carbon Fiber Reinforced Epoxy: CFRP

A commercial epoxy resin (TETRED-X), N.N.N'.N'-tetra-glycidyl-methoxy-diamin, from Mitsubishi Gas Chemical Co., was used as a composite matrix. The curing agent added in this experiment was 1,2 cyclo-hexane-dicarboxylic anhydride (HHPA) from Wako Junyaku company. The weight ratio of TGMXDA to

HHPA was 100 : 131. PAN based carbon fiber manufactured by Toho Rayon Co. Ltd. (Tokyo, Japan) was selected as the fiber reinforced component in this experiment. Physical properties of this fiber are shown in Table 1.

The normal FRP consisting of 30% to 50% carbon fiber and epoxy resin, CFRP, was fabricated by a filament-winding technique. Unidirectional fibers were pulled through the resin bath (a mixture of epoxy and hardener) and wound onto a mandrel (100 mm in diameter) at a speed depending upon the volume fraction of fiber content in the composite. After winding onto the mandrel was complete, fiber/epoxy flat sheets were cut into 100 x 100 mm segments and stacked one upon another. The cut sheets were then transferred into a press machine and pressed at 1.3 MPa with pre-curing at 90°C for 2 hr. After pre-curing, the press-mold was post-cured at 180°C for 2 hr. Composites were then cut into 80 x 8 x 2 mm pieces and ground for mechanical tests.

with two kinds of Al_2O_3 filler using wet-ball milling in ethanol for 12 hours. Homogeneous dispersion of 10% Al_2O_3 filler into the epoxy matrix was achieved by this ball milling method. Solvent was then evaporated and hardener was added. After mixing well with the hardener, the epoxy resin bath was filled with the mixture of epoxy/hardener and 10 vol% of Al_2O_3 filler. This CFHRP with two types of Al_2O_3 filler was also prepared by filament winding. The rest of the procedure was the same as for CFRP fabrication.

2.3. Characterization of Composites

The mechanical properties, Young's modulus, interlaminar shear strength, and deformation behaviors were evaluated for CFRP and Al_2O_3 particle dispersed CFHRP composite. Young's modulus was measured using the flexural vibration resonance method at room temperature. Interlaminar shear strength was determined according to ASTM D-2344. Five specimens

Table 1
Physical properties of carbon fiber used in this experiment

Property	units
Diameter	7μm
Young's modulus	235(Gpa) Lonitudinal direction
Young's modulus	16(Gpa) Transverse direction
Tensile strength	3720(Mpa)
Elongation at break	1.6%
Density	1.77 g/cm3
Electrical resistivity	1.5x10-3 ohm cm

2.2. Hybrid Carbon Fiber Reinforced Epoxy: CFHRP

In the experiment γ-Al_2O_3 (Asahi Chemical Co. Japan) particles with an average particle size of 25 nm and α-Al_2O_3 (Sumitomo Chemical Co. Japan) with an average particle size of 1 μm were dispersed into epoxy matrix for hybrid CFRP (CFHRP). Epoxy resin was mixed

were used for determination of each mean value.

Deformation/fracture behaviors of carbon fiber and epoxy resin(:CFRP) and 10% Al_2O_3 particle dispersed CFHRP composites with carbon fiber content of 20 to 50% were evaluated by monitoring by the Ultra-Micro-Indentor (UMIS-2000, from Cisro, Australia) using the Berkovich type (triangular diamond pyramid) indentor

/9/. Continuous loading-unloading indentations to 30 mN of indent load were carried out on the polished surface section normal to the fiber axis of CFRP and Al_2O_3 particle dispersed CFHRP. Elastic modulus was calculated from the slope fitted to the upper one-third portion of unloading compliance data.

SEM and optical microscopic observation was performed to investigate the fracture behavior, fiber matrix adhesion/bonding, fiber matrix interface, fracture nature of carbon fiber, and fiber pullout.

3. RESULTS AND DISCUSSION

Young's Modulus (*longitudinal direction*)

Fig. 1 shows the variation of Young's modulus in the longitudinal direction with a function of fiber content for CFRP and CFHRP with micron-size Al_2O_3 particles (M-CFHRP) and nano-size Al_2O_3 particles (N-CFHRP). Young's modulus of all composites increased with increasing fiber content. The experimental results were found to agree well with the results calculated from the linear rule of mixing, for both CFRP and CFHRP composites. Young's modulus of the composites increased with the addition of filler. It was also seen from Fig. 1 that N-CFHRP showed a higher modulus than CFRP and M-CFHRP. Thus an improvement in the modulus is mainly caused by the improvement of matrix modulus by filler dispersion, i.e., load transfer.

Young's Modulus (*transverse direction*)

The relationship between fiber content and Young's modulus in the transverse direction of CFRP, M-CFHRP and N-CFHRP is shown in Fig. 2. It is well known that the Young's modulus of carbon fiber in the transverse direction is lower (16 GPa) than that in the longitudinal direction (234 GPa). In general, Young's modulus in the transverse direction depends mainly on the modulus of the matrix, although the Young's modulus of CFRP in the longitudinal fiber direction depends on the modulus of the fiber and the matrix. Young's modulus of these composites was found to

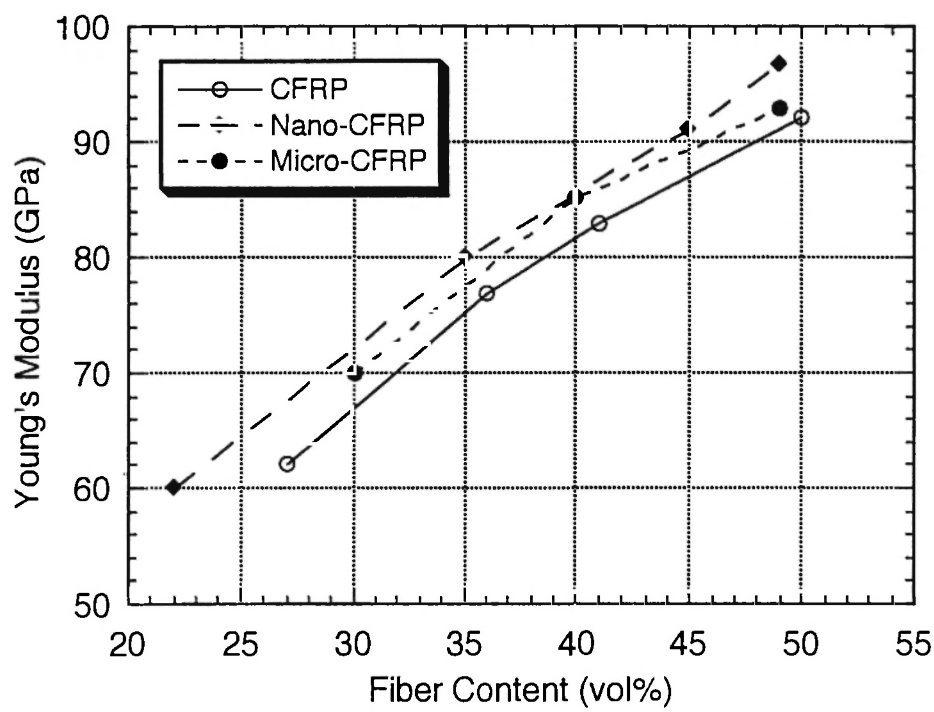

Fig. 1: Young's modulus (longitudinal direction) as a function of fiber content for CFRP, M-CFHRP and N-CFHRP.

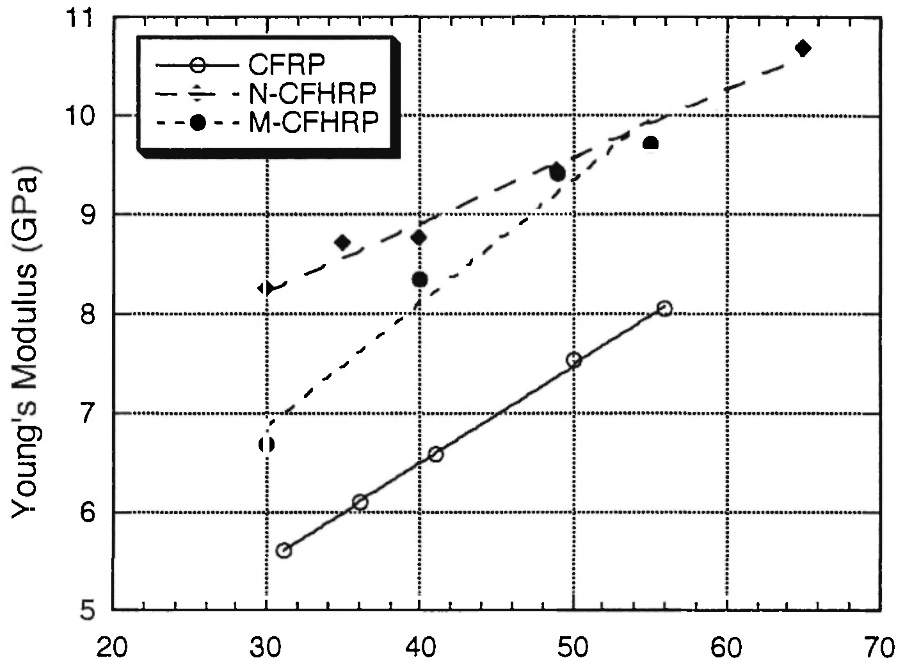

Fig. 2: Young's modulus (transverse direction) as a function of fiber content for CFRP, M-CFHRP and N-CFHRP.

agree well with the rule of mixture calculated by the following equation:

$$1/E_c = V_f/E_f + (1-V_f)/E_m'$$

where $E_m' = E_m/1-\nu^2$, E_c refers to the modulus of the composites, V_f is volume fraction of fiber, E_m and E_f is the Young's modulus of matrix and fibers respectively /1,11/. A small deviation from the theoretical value is thought to be due to fiber misorientation and overlapping of fibers. Dispersion of Al_2O_3 filler particles into the epoxy matrix of CFRP also improved the Young's modulus value remarkably. This increase of Young's modulus for M-CFHRP and N-CFHRP is explained by the increase of Young's modulus of matrix which was due to load transfer caused by the addition of rigid high modulus filler into epoxy. Furthermore, as clearly shown in Fig. 2, the improvement was observed to be higher for dispersed nano-size Al_2O_3 filler compared to micron-size filler. Our previous papers reported that the incorporation of nano-size rigid filler particles into the epoxy matrix improved the Young's modulus of epoxy remarkably /12,13/. Recently it has been reported that Young's modulus of epoxy matrix depends on the filler size dispersion and the local stresses caused by the thermal mismatch between epoxy and filler in the composites matrix, which are dependent on the distance between each particle /14/. Because the addition of finer filler is expected to increase the volume of local stress field, compared to the addition of coarse filler, nano-size Al_2O_3 filler dispersed CFHRP shows the highest modulus, due to both the load transfer effect and the increase of local stresses caused by the thermal mismatch between epoxy and filler.

Interlaminar Shear Strength: ILSS

The effect of carbon fiber content on interlaminar shear strength (ILSS) of CFRP, M-CFHRP and N-CFHRP is shown in Fig. 3. It was observed that ILSS value increased with increasing fiber content for CFRP and M-CFHRP. Although the ILSS value showed the maximum at 35 vol% fiber content with the addition of nano-size Al_2O_3 particles to the CFRP composites, N-

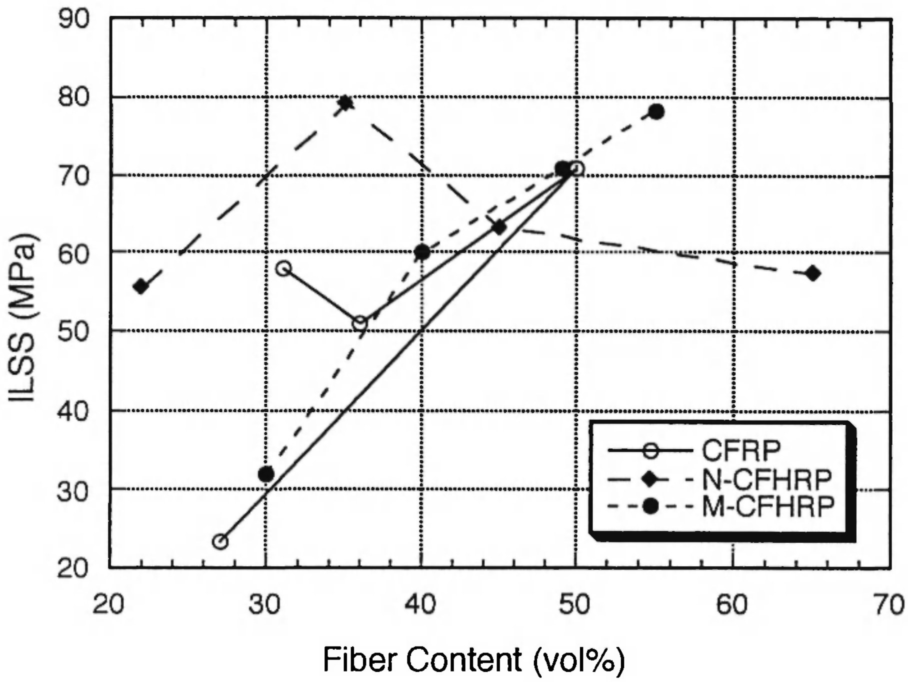

Fig. 3: ILSS as a function of fiber content for CFRP, M-CFHRP and N-CFHRP.

CFHRP possessed the constant ILSS over 40 vol% of fiber content. This degradation of ILSS of N-CFHRP was caused by the agglomeration of nano-size filler. This increase in ILSS of M-CFHRP and N-CFHRP is thought to be due not only to the improvement of matrix strength by load transfer but also to the bonding and strength at fiber/matrix interface enhanced by filler dispersion. Any change in thermal shrinkage/residual stresses between epoxy matrix and fiber creates pressure at the fiber surface, which leads to the strong adhesion between the fiber and matrix. For single fiber inclusion in the matrix, interface pressure (P) can be shown by the following equation:

$$P = \frac{(\alpha_m - \alpha_f)\Delta T E_m}{(1+\upsilon_m)+(1-\upsilon_f)E_m / E_f}$$

where P is the interface pressure caused by thermal shrinkage of epoxy material while cooling, α_m is the coefficient of thermal expansion of matrix, α_f is coefficient of thermal expansion of fiber, ΔT is the temperature difference between T_g and room temperature, υ_f is the Poisson ratio of fiber, E_m the elastic modulus of matrix and E_f the elastic modulus of carbon fiber /15/. Using the above equation, interface pressure was calculated to be 36.2 MPa, 43.7 MPa and 51.9 MPa for CFRP, M-CFHRP and N-CFHRP, respectively. This increase of interface pressure leads to the increase of Young's modulus caused by load transfer by addition of rigid filler and the difference of thermal mismatch between epoxy and filler, as mentioned above in the section on Young's modulus. As this increase of interface pressure, especially in the radial direction, achieves the enhancement of friction shear stress, τ_f, the improvement of ILSS for CFHRP was thought to be achieved. Therefore, it was revealed that the addition of ceramic filler into epoxy matrix achieves the synergy effect of increase in Young's modulus and the improvement of bonding and strength at fiber/matrix interface caused by filler dispersion.

Microscopic Deformation by UMIS

Fig. 4 shows the typical result of penetration depth

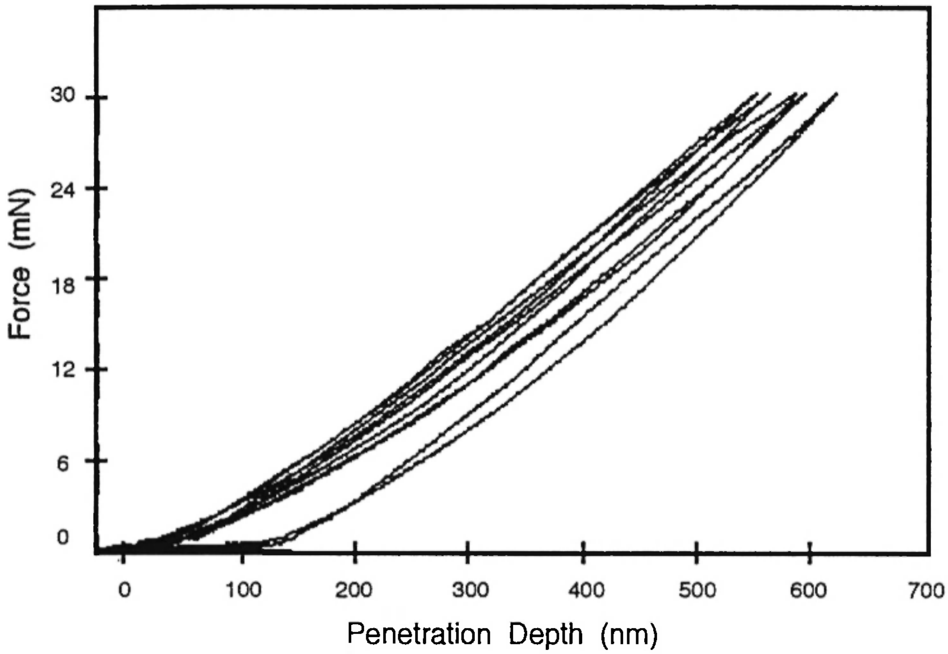

Fig. 4: Typical profile of penetration depth with increasing load indented by the Berkovich /9/.

profile when indented load is increased by UMIS. In order to confirm the change of constraint condition, macroscopic deformation of carbon fiber was studied. The Berkovich indentations, which are the penetration of a triangular diamond pyramid /9/ were penetrated on the fiber in the epoxy matrix with a load of 30 mN. This UMIS can monitor the relation of load and penetration depth with stepping load of 1.5 mN/step and analyze the deformation/fracture behavior of the matrix and fiber indented /9/. At least five indentations were performed in this experiment.

CFHRP and N-CFHRP after penetration of 30 mN by the Berkovich indentor is shown in Fig. 5. The plastic deformed depth of CFHRP was decreased by the addition of filler to the epoxy matrix. Using these deformation depth data, hardness at maximum depth was calculated. The changes of hardness for CFRP, M-CFHRP and N-CFHRP are shown in Fig. 6. Both M-CFHRP and N-CFHRP showed more hardness than CFRP. N-CFHRP showed the highest hardness, which was approximately 1.5 times that of CFRP. The reason for the hardness enhancement is thought to be that the friction force at the interface of fiber and matrix was

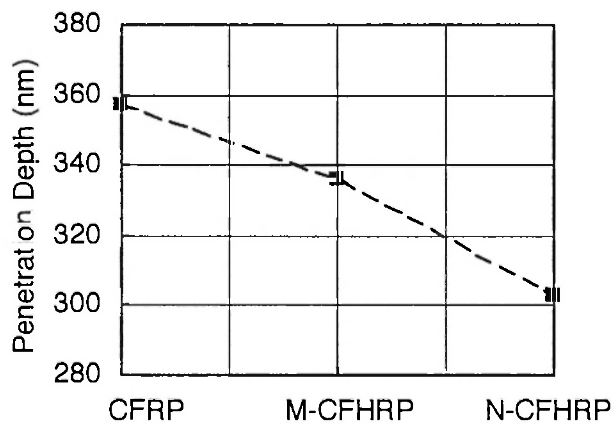

Fig. 5: Final depth of plastic deformation of carbon fiber for CFRP, M-CFHRP and N-CFHRP.

increased by local stresses caused by the thermal mismatch between epoxy and filler.

Fig. 7 shows the Young's modulus of carbon fiber for CFRP, M-CFHRP and N-CFHRP. Young's modulus of M-CRHRP and N-CFHRP showed higher values than CFRP. These results agree well with the above-mentioned results of Young's modulus of CFRP and

CFHRP in the transverse direction using the flexural vibration resonance method. It is thought that this increase of Young's modulus with the addition of filler to CFRP can be attributed to the increase of local stresses at the interface of fiber and matrix caused by the thermal mismatch between epoxy and filler. The addition of nano-size Al_2O_3 filler therefore enhanced the Young's modulus markedly.

These results suggested that the resistance against the penetration increased with the addition of filler, especially with the addition of nano-size Al_2O_3 filler. According to the analyses by UMIS, the hybridization of the nano-size filler dispersed CFRP is thought to be effective for improvement of mechanical properties in the transverse direction of reinforcement fiber, which is attributed to the change of constraint condition of carbon fiber due to the filler dispersion. A study of the precise mechanism of increase in Young's modulus and hardness is in progress.

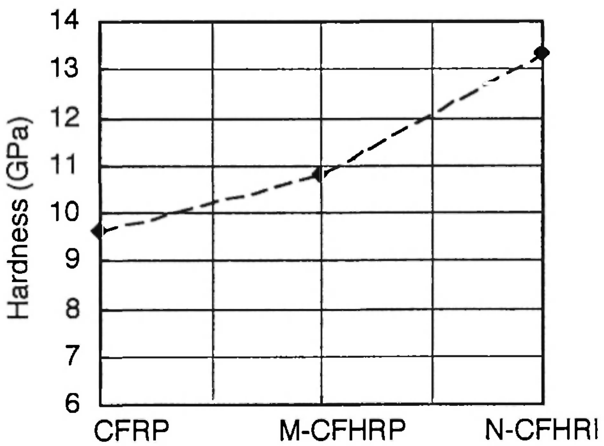

Fig. 6: Hardness of carbon fiber for CFRP, M-CFHRP and N-CFHRP.

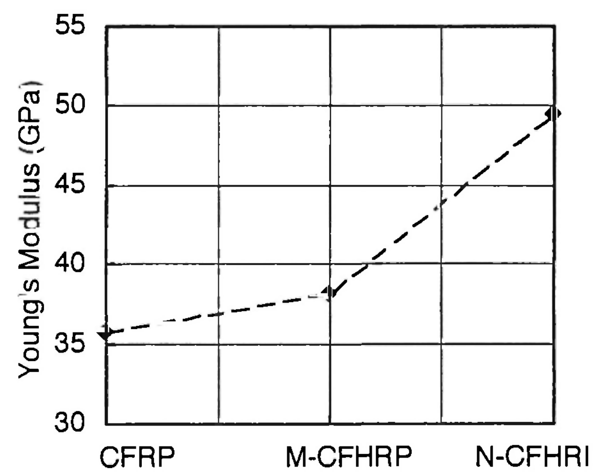

Fig. 7: Young's modulus of carbon fiber for CFRP, M-CFHRP and N-CFHRP.

4. SUMMARY

The mechanical properties of fibers in the transverse direction, such as Young's modulus and interlaminar shear strength, were significantly enhanced by incorporation of 10 vol% Al_2O_3 filler, especially nano-size Al_2O_3 particulate. By UMIS, the relation of load and penetration depth and the deformation/fracture behavior of fiber in the matrix on the surface section normal to fiber axis was studied. These results suggested that hybridization of the epoxy matrix fiber reinforced by nano- or micro-size Al_2O_3 fillers is effective for improvement of mechanical properties of CFRP, which is attributed to the change of constraint condition of carbon fiber. For practical applications high stiffness FRP composites are desired; thus the only way to improve the Young's modulus and hardness of FRP is to improve the modulus properties of matrix by incorporating rigid filler into the matrix, especially nano-size filler.

REFERENCES

1. J. Ki, and Y.W. Mai, *J. Mater. Sci.*, **26**, 4702 (1991).
2. S. Saiello, J. Kenny and L. Nicolais, *J. Mater. Sci.*, **25**, 3493 (1990).
3. J.K. Wells and P.W.R. Beaumont, *J. Mater. Sci.*, **23**, 1274 (1988).
4. N. Melanit, C. Galiotis, P.L. Tetlow and C.K.L. Davies, *J. Mater. Sci.*, 28, 1648 (1993).
5. H.J. Sue, R.E. Jones and E.I.G. Meitin, *J. Mater. Sci.*, **228**, 6381 (1993).
6. K.P. Gadkaree, *J. Mater. Sci.*, **27**, 3827-3834 (1992).

7. L.M. Manocha, *J. Mater. Sci.*, 17, 3039 (1982).
8. L. Di Landro and M. Pegoraro, *J. Mater. Sci.*, **22**, 1980 (1987).
9. R.D. Dukino and M. Swain, *J. Am. Ceram. Soc.*, **75**, 3299 (1992).
10. S.W. Tsai, AMFL-TR66-149 (1966).
11. R.M. Jones, *Mechanics of Composite Materials*, McGraw-Hill, 1975.
12. M. Hussain, Y. Oku, A. Nakahira and K. Niihara, *Ceramic Transactions*, 44, 409 (1994).
13. M. Hussain and K. Niihara, *Proc. 4th Int. SAMPE Symp.*, 1995; p. 386.
14. M. Hussain, A. Nakahira, S. Nishijima and K. Niihara, *Materials Letters*, in press, 1996.
15. G. Gerard and A.C. Gilbert, *J. Appl. Mech. ASME*, **24**, 355 (1957).